A Letters Journal Exploring the Frontiers of Physics

February 2008

EPL, **81** (2008) 46003
doi: 10.1209/0295-5075/81/46003

www.epljournal.org

Experimental evaluation of apparent tissue surface tension based on the exact solution of the Laplace equation

C. Norotte[1], F. Marga[2], A. Neagu[2,3], I. Kosztin[2(a)] and G. Forgacs[1,2(b)]

[1] *Department of Biological Sciences, University of Missouri - Columbia, MO 65211, USA*
[2] *Department of Physics and Astronomy, University of Missouri - Columbia, MO 65211, USA*
[3] *Department of Biophysics and Medical Informatics, University of Medicine and Pharmacy Timisoara 300041 Timisoara, Romania*

received 23 October 2007; accepted in final form 20 December 2007
published online 24 January 2008

PACS 68.03.Cd – Surface tension and related phenomena
PACS 87.17.-d – Cellular structure and processes

Abstract – The notion of apparent tissue surface tension offered a systematic way to interpret certain morphogenetic processes in early development. It also allowed deducing quantitative information on cellular and molecular parameters that is otherwise difficult to obtain. To accurately determine such tensions we combined novel experiments with the exact solution of the Laplace equation for the profile of a liquid drop under the employed experimental conditions and used the exact solution to evaluate data collected on tissues. Our results confirm that tissues composed of adhesive and motile cells indeed can be characterized in terms of well-defined apparent surface tension. Our experimental technique presents a way to measure liquid interfacial tensions under conditions when known methods fail.

In the absence of external forces, embryonic tissue fragments round up. Cells of two distinct tissues randomly intermixed within a single multicellular aggregate sort into separate regions. To account for such liquid-like phenomena Steinberg introduced the notion of apparent tissue surface tension. This quantity provides a measure to physically characterize tissue composed of motile cells with distinct adhesive apparatus. According to the differential adhesion hypothesis (DAH), on the other hand, differences in adhesion drive certain morphogenetic processes in early embryonic development [1,2]. Predictions of DAH have been confirmed both *in vitro* [3] and *in vivo* [4–6]. The apparent surface tensions of different embryonic tissues (*i.e.* interfacial tensions with the surrounding culture medium) were measured and the values accounted for the observed mutual sorting behavior [3,7]. Importantly, since surface tension is a measure of the liquid's cohesivity, in the case of tissues it should be related to molecular parameters. Indeed, it was shown on theoretical grounds that $\sigma \propto JN$, where J and N are, respectively, the bond energy between two homotypic cell adhesion molecules (CAMs) and the surface number density of CAM [8]. The linear dependence of the surface tension σ on N has recently been confirmed experimentally [9]. Despite these analogies, it has to be emphasized that tissues are not liquids. The movement of loosely bound liquid particles is driven by van der Waals forces and powered by thermal energy with scale set by kT (k —Bolzmann constant, T —absolute temperature). On the other hand the motion of cells bound in tissues by cell adhesion molecules (CAMs) or substrate adhesion molecules is powered by metabolic energy, with scale set by ATP hydrolysis. Apparent tissue surface tension however provides a useful means to systematically interpret equilibrium cellular arrangements and distinguish between tissues containing motile and adhesive cells.

Currently, the only available method to measure σ for submillimeter size tissue aggregates is by compression plate tensiometry [7,8,10]. The method, based on the Laplace equation, so far relied on various approximations of the geometrical profile of an equilibrated spherical aggregate compressed between two parallel plates and yielded σ values that can at best be considered relative and their independence on aggregate size and compressive force questionable.

The motivation for the present work was to establish a method by which the absolute values of apparent tissue

(a) E-mail: kosztini@missouri.edu
(b) E-mail: forgacsg@missouri.edu

surface tensions can accurately and reliably be determined and thus used to obtain biologically relevant information on molecular quantities (such as J). To accomplish these objectives we exactly solved the Laplace equation for the profile of a droplet under the geometric conditions of compression plate tensiometry. The analytic solution allows to express σ in terms of easily and accurately measurable geometric parameters. On the experimental side we extended the method to the simultaneous compression of several droplets of different size and with this considerably improved on the measurement statistics. When tested on true liquids the method reproduced earlier results on σ. Our findings on tissues and multicellular aggregates indicate that these systems are incompressible and their σ's are independent of the magnitude of the compressive force and the volume of the aggregates. These results provide strong evidence for the concept of tissue surface tension and support its usefulness for the interpretation of early morphogenetic processes. They furthermore illustrate the power of analogies (a commonly used approach in physics), in the present case, to obtain valuable information on the molecular level from biophysical measurements performed at the multicellular level.

For a small liquid droplet compressed between two parallel plates σ can be determined from its geometric shape (fig. 1A,B). We consider droplets with radius R_0 smaller than the millimetric capillary length $R_c \approx (\sigma/\rho g)^{1/2}$, for which the effect of gravity can be neglected. (For water $R_c \approx 2.6\,\mathrm{mm}$, while for cellular aggregates considered here $R_c > 1\,\mathrm{mm}$.) The shape of such a liquid drop placed on a horizontal plate (fig. 1A) is a spherical cap of radius R_{10} and height H_0. In terms of these parameters, the (external) contact angle $\theta = \cos^{-1}(H_0/R_{10} - 1)$ and, assuming incompressibility, the radius of the suspended drop, $R_0 = R_{10}[(2-\cos\theta)\cos^4(\theta/2)]$. While H_0 and R_{10} can be measured with high accuracy (*e.g.*, $\sim 1\%$), the relative error $\Delta\theta/\theta \approx [(1+\cos\theta)/\theta\sin\theta](\Delta H_0/H_0 + \Delta R_{10}/R_{10})$ can still be very large (*e.g.*, $\gg 130\%$ for $\theta < 10^\circ$). Thus, to accurately determine σ it is desirable to avoid using quantities that explicitly contain the contact angle.

The compressed drop has rotational symmetry about the z-axis and reflection symmetry with respect to its equatorial plane, in which it has the two principal radii of curvatures R_1 and R_2 shown in fig. 1B. R_3 is the radius of the droplet's circular area of contact with the compression plates. The magnitude of compression depends on the compression force F applied to the upper (or lower) plate. In terms of R_1 and R_2 the excess pressure inside the drop due to the surface tension is given by the Laplace formula $\Delta p = \sigma(1/R_1 + 1/R_2)$. For the system formed by the upper plate and the portion, of thickness h $(0 \leqslant h \leqslant H/2)$, of the compressed drop situated between the plate and an arbitrary horizontal boundary plane, at mechanical equilibrium, the vector sum of the compression force, hydrostatic force (due to the excess pressure) and the surface tension force vanishes. This equilibrium condition,

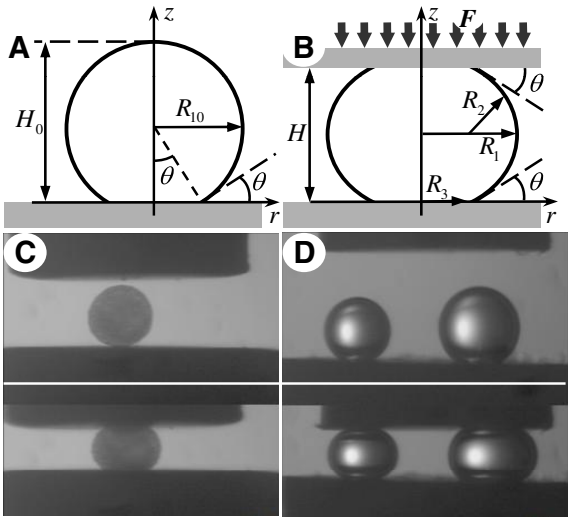

Fig. 1: Schematic diagram of an (A) uncompressed and (B) compressed liquid drop. (C) Snapshots of uncompressed (top) and compressed (bottom) cushion tissue (CT) spheroids in culture medium. (D) Same for water drops in olive oil (W-O). The diameter of the uncompressed CT and the smaller W-O drops were 0.402 mm and 0.441 mm, respectively.

when evaluated along the vertical axis, implies $F = \Delta p A - \sigma\ell\sin\varphi$. Here A and ℓ are, respectively, the cross-sectional area and the perimeter of the liquid drop in the boundary plane, and φ is the angle between the horizontal and the tangent to the profile of liquid drop at the boundary plane. For $h = 0$ (*i.e.*, the horizontal boundary plane located just underneath the upper plate), $A = \pi R_3^2$, $\ell = 2\pi R_3$ and $\varphi = \theta$. Thus, by using the Laplace formula for Δp, one obtains

$$F = \pi\sigma\left[R_3^2(1/R_1 + 1/R_2) - 2R_3\sin\theta\right]. \tag{1a}$$

Similarly, for $h = H/2$ (*i.e.*, the horizontal boundary plane coinciding with the median plane of the compressed drop), one has $A = \pi R_1^2$, $\ell = 2\pi R_1$ and $\varphi = \pi/2$, and as a result

$$F = \pi\sigma R_1(R_1/R_2 - 1). \tag{1b}$$

In addition to H, R_1 and F (which can be accurately measured), to determine σ directly from either of these two equations, requires the quantities R_2, θ and R_3 that can only be measured with large errors. In earlier studies this problem has been circumvented by assuming $\theta = 0$ (no adhesion to the plates) and/or making approximations on the lateral profile of the drop, *e.g.*, $R_3 = R_1 - R_2$ (the profile is a semicircle) or $R_3 = R_1 - R_2 + [R_2^2 - (H/2)^2]^{1/2}$ (the profile is a circular arc) [3,8]. Each of these schemes fails to give consistent results in some range of the compressive force or contact angle. For example, approximating the lateral profile with a circular arc implies that the contact angle depends on the magnitude of the compressive force, an unphysical conclusion.

To determine R_1, R_2 and R_3 requires the exact profile $z(r)$ of the compressed liquid droplet, which can be

obtained by the exact integration of the Laplace equation

$$\Delta p = \sigma \left[\frac{z'}{r(1+z'^2)^{1/2}} + \frac{z''}{(1+z'^2)^{3/2}} \right] = \text{const}, \quad (2)$$

subject to the boundary conditions (see fig. 1B)

$$\begin{aligned} z(R_3) &= 0, & z'(R_3) &= \tan\theta, \\ z(R_1) &= H/2, & z'(R_1) &= \infty\,. \end{aligned} \quad (3)$$

The terms in the square brackets in eq. (2) represent the principal curvatures of the drop's surface at a point determined by $z(r)$. In the above equations z' and z'' represent the first and second derivatives of the function $z(r)$.

We are now in the position to determine σ in terms of the easily and accurately measurable quantities H, R_1 and F. Equations (1) imply that both R_2 and R_3 can be expressed in terms of R_1

$$R_2 = R_1/(2\alpha - 1)\,, \quad R_3 = \beta_\theta R_1\,, \quad (4a)$$

where the dimensionless parameters α and β_θ are given by

$$\alpha = \Delta p/(2\sigma/R_1)\,, \quad (4b)$$

$$\beta_\theta \equiv \beta_\theta(\alpha) = \frac{\sin\theta + \sqrt{\sin^2\theta + 4\alpha(\alpha-1)}}{2\alpha}\,. \quad (4c)$$

Integrating eq. (2) with the boundary conditions (3) leads to an implicit equation for α

$$\begin{aligned} \frac{H}{2R_1} &= f_\theta(\alpha) \equiv \int_{\beta_\theta}^{1} z'(x)\mathrm{d}x\,, \\ z'(x) &= \left[\left(\frac{x}{\alpha x^2 + 1 - \alpha} \right)^2 - 1 \right]^{-1/2}, \end{aligned} \quad (5)$$

and the lateral profile of the compressed drop

$$z(r) = R_1 \int_{\beta_\theta}^{r/R_1} z'(x)\mathrm{d}x. \quad (6)$$

The α-dependence of the functions $f_\theta(\alpha)$ and $\beta_\theta(\alpha)$ is shown in fig. 2 for several values of the contact angle (*i.e.*, $\theta = 0°, 10°, \ldots, 40°$). By simple inspection one can see that $\beta_\theta(\alpha)$ has a much stronger θ-dependence than $f_\theta(\alpha)$. In fact, one finds that $f_\theta(\alpha) \approx f_0(\alpha)$ is an excellent approximation for $\theta \leqslant 20°$. Thus, for small contact angles, it follows that $\alpha = f_0^{-1}(H/2R_1)$ and, therefore, R_2 are relatively insensitive to even large (*e.g.*, $\sim 10°$) sample-to-sample fluctuations of θ (*e.g.*, caused by local inhomogeneities or impurities). By contrast, since β_θ itself strongly depends on θ, so does R_3. This explains why its determination by fitting the lateral profile of the drop by circular arcs leads to sizable errors.

Finally, σ can be expressed from either eq. (1a) or (1b), which in terms of $\alpha = f_\theta^{-1}(H/2R_1)$ (see eq. (5) and fig. 2a) can be rewritten as

$$F/2\pi R_1 = \sigma(\alpha - 1). \quad (7)$$

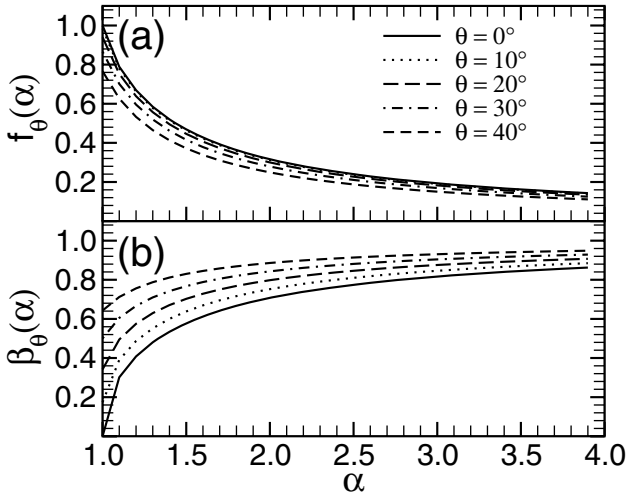

Fig. 2: Plot of (a) $f_\theta(\alpha)$, and (b) $\beta_\theta(\alpha)$ for different values of the contact angle θ.

For sufficiently weak adhesion between the liquid drop and compression plates (*i.e.*, $\theta \leqslant 20°$), this result provides a simple recipe to evaluate σ from the measurement of only H, R_1 and F. Namely, σ is given by the slope of the least square linear fit to the experimentally measured data points $\{f_0^{-1}(H/2R_1) - 1,\, F/2\pi R_1\}$, that goes through the origin. The efficiency of the proposed method for measuring σ can be further enhanced by simultaneously compressing several ($n = 1, \ldots, N$) drops, as shown in fig. 1D. For such compressions the quantities $F/2\pi R_1$ and α in eq. (7) need to be replaced, respectively by $F/2\pi\bar{R}_1$ and $\bar{R}_1^{-1}\sum_n R_{1n}\alpha_n$, with $\bar{R}_1 = \sum_n R_{1n}$ and $\alpha_n = f_0^{-1}(H/2R_{1n})$.

It should be emphasized that eq. (5) is valid for incompressible and compressible liquids alike. For incompressible liquids volume conservation yields

$$(R_0/R_1)^3 = g_\theta(\alpha) \equiv (3/2)\int_{\beta_\theta}^{1} x^2 z'(x)\mathrm{d}x. \quad (8)$$

Similarly to the function $f_\theta(\alpha)$, for $\theta \leqslant 20°$, one finds that to a very good approximation $g_\theta(\alpha) \approx g_0(\alpha)$. Eliminating α between eqs. (5) and (8) leads to

$$H/2R_1 = U_\theta(H/2R_0) \approx U_0(H/2R_0), \quad (9)$$

where U_0 is a universal function defined through: $U_0(x) = f_0(\alpha)$ and $x = f_0(\alpha)[g_0(\alpha)]^{1/3}$. Thus, for weak adhesion between the drop and plates (*i.e.*, $\theta \leqslant 20°$) there is a universal relationship between $H/2R_1$ and $H/2R_0$, valid for any incompressible liquid drop regardless of its type or size.

We have tested the above theory to determine the interfacial tension of true immiscible liquids (water in olive oil (W-O) and turpentine (W-T)), where results obtained by other methods are available. Subsequently, we applied the analytical results to obtain the absolute values of tissue surface tensions. Measurements were performed using a

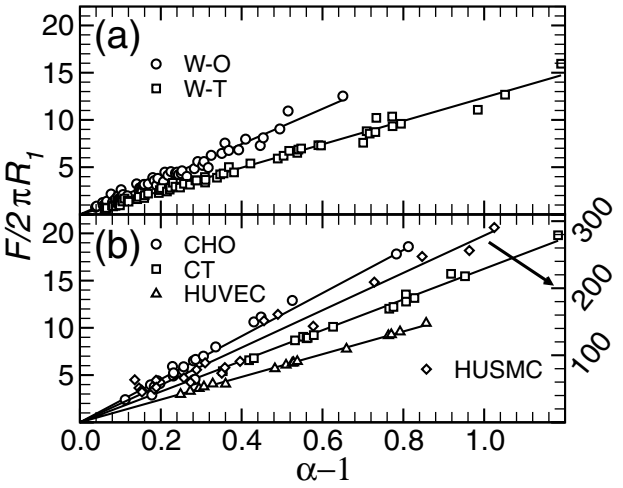

Fig. 3: Employing eq. (7) for data evaluation. The surface and interfacial tensions are obtained from the slopes of the linear fit to the data points including the origin: (a) pure liquid (W-O, W-T), and (b) tissues and multicellular aggregates (CT, CHO, HUVEC, HUSMC). As indicated by the arrow, the vertical axis on the right corresponds to HUSMC.

Table 1: Interfacial tensions (in case of tissues and cell aggregates between the biological material and the surrounding culture medium) of the studied systems obtained from the data shown in fig. 3. The absolute errors $\Delta\sigma$ are standard deviations. The last two columns contain respectively the percentage relative errors and the number of data points.

System	σ (mN/m)	$\Delta\sigma$ (mN/m)	$\Delta\sigma/\sigma$ (%)	Data points
W-O	18.6	2.4	12.9	56
W-T	12.4	1.5	12.1	60
CHO	22.8	3.0	13.2	22
CT	16.3	0.2	1.2	17
HUVEC	12.0	0.2	1.7	16
HUSMC	279	57	20.4	21

specifically designed compression tensiometer (for details see [10]). In the case of ordinary liquids compressions were performed on one or simultaneously two spherical water drops of various size (ranging from 0.4 to 1 mm in diameter) (fig. 1D). In each experiment, drops were exposed to at least 3 successive compressions (up to 9) of increasing force and their profile was recorded at shape equilibrium.

For biological measurements we either used intact tissue (fragments of excised embryonic chicken cardiac cushions (CT) that round into spheres in about 12 hours) or spherical aggregates composed of various cell types, such as Human Umbilical Smooth Muscle Cells (HUSMC), Human Umbilical Vein Endothelial Cells (HUVEC) and Chinese Hamster Ovary cells (CHO)). The three cell lines were chosen to sample cells with strongly differing biological function. Aggregates were prepared as previously described [10]. Briefly, confluent cell cultures were detached from the Petri dish. Cell solutions were subsequently centrifuged and the resulting pellets transferred into capillary micropipettes of 300 and 500 μm diameter and incubated at 37 °C with 5% CO_2 for 15 minutes. The firm cylinders of cells removed from the pipettes were cut into 250–600 μm long fragments (to arrive at cylinders with aspect ratio close to 1), then incubated on a gyratory shaker with 5% CO_2 at 37 °C for 24–36 hours. This protocol reproducibly produced spherical aggregates of similar size. Tissue spheroids were compressed in culture medium at 37 °C (fig. 1C). One to six spheroids of each type were compressed simultaneously. In order to avoid irreversible damage to the cells, no more than 2 compressions were performed on any one spheroid.

Upon compression cellular aggregates relax to equilibrium in a manner typical for viscoelastic materials [8]. As demonstrated earlier, by the end of this relaxation process the initially compressed cells regain their pre-compressed shape [11]. Since compression leads to the increase of the surface area, provided volume remains the same, this finding implies that cells from the interior of the aggregate have to migrate to the surface.

According to equation (7), for liquids, the pairs of data points $\{(\alpha-1), F/2\pi R_1\}$ should lie on a straight line passing through the origin, with σ given by the slope of the line. The data is shown in fig. 3 and the obtained results are summarized in table 1. In addition to the values of σ, the table also contains the standard deviation ($\Delta\sigma$), the corresponding percentage relative errors ($\Delta\sigma/\sigma$) and the total number of data points used in fig. 3. Results for W-O (18.6 ± 2.4 mN/m) and W-T (12.4 ± 1.5 mN/m) compare well with published data [12] (17 mN/m and 13.7 mN/m, respectively). The corresponding relatively large errors ($\sim 12\%$) in table 1 reflect the sample sensitivity of σ and not a deficiency of the method. Indeed, the large number of W-O and W-T compression measurements (see table 1) were done in the course of four days, each time using different samples and compression plates. Most of these experiments were carried out on single droplets, which might have experienced somewhat different environmental conditions (sample-to-sample fluctuations). The actual errors $\Delta\sigma$ corresponding to drops from the same batch were much smaller ($\sim 1\%$). Another possible source of error is related to the extent of compressions. Weaker compressions result in larger errors. From eq. (7), $\Delta\sigma/\sigma = \Delta F/F + \Delta R_1/R_1 + \Delta\alpha/(\alpha-1)$ which may become large when $F \to 0$ and $\alpha \to 1$.

For tissue fragments and cell aggregates σs were determined by a similar procedure, with the results shown in fig. 3b and table 1, which clearly demonstrate that embryonic tissues and cell aggregates have well defined (apparent) surface tensions that are independent of their size or extent of compression. Measurements on CT and HUVEC were carried out with simultaneously prepared spheroids, which explains the small $\Delta\sigma$. These spheroids were exposed to multiple multi-aggregate compressions: five or six aggregates compressed twice. CHO aggregates

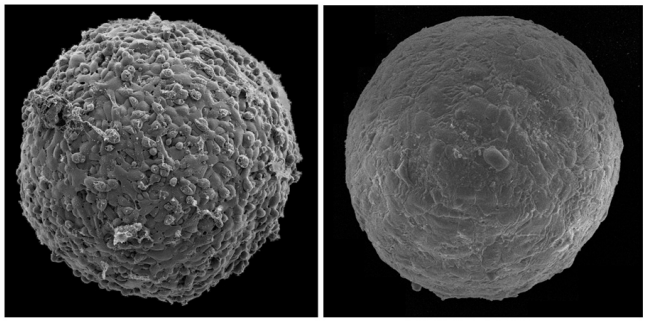

Fig. 4: Scanning electron microscopy images of CHO (left) and HUSMC (right) cell aggregate surfaces. The berry-like shape of many of the CHO cells reveals limited adhesion between surface and subsurface cells. The flattened shape of HUSMCs implies that they strongly adhere to subsurface cells. These surface morphologies are consistent with the measured values of the corresponding surface tensions. The diameter of the shown aggregates is about 500 micron.

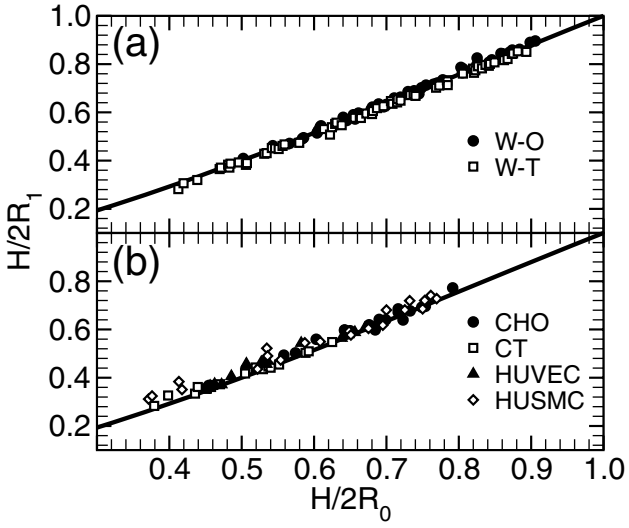

Fig. 5: Testing incompressibility through the universal function given in eq. (9) (solid curve) to assess the incompressibility of the (a) liquid and (b) tissue and multicellular spheroids used in the compression measurements.

also originated from a single batch, but compressions were performed on both single and multiple (two to five) aggregates, resulting in error similar to that of W-O and W-T. For HUSMC four different batches of aggregates were used and, due to the large forces needed, only single aggregate compressions were performed. This may explain the relatively large error ($\sim 20\%$). The above results on the values of the tensions suggest that multi-aggregate compressions with aggregates from a single batch is the most accurate way of experimentally determining σ. In light of the earlier discussed relationship between tissue surface tension and the intensity of binding between the constituent cells, our results suggest that smooth muscle cells adhere to each other with considerably greater strength than the other cell types studied here. This suggestion is further supported by fig. 4. The strong adhesion between smooth muscle cells may be consistent with their physiological role. These cells reside within the walls of hollow organs (*e.g.* bladder, vasculature) that are exposed to great mechanical load. Whereas it is well demonstrated that most of the arterial wall stress is supported by collagen fibers, it is also known that upon arterial wall injury, smooth muscle cells quickly migrate and proliferate at the lesion site. Thus one can hypothesize that, because of their high cohesion (the strongest that has ever been measured on a tissue or cell type by tensiometry), they act as a first barrier (or "glue") to preserve the physical integrity of the vascular wall.

The fact that the data points $\{H/2R_0, H/2R_1\}$ for all our measurements fall on the universal curve predicted by eq. (9) (fig. 5) confirms that the multicellular systems studied here, similarly to water, are incompressible and provides an additional validation for our method.

In summary, our results convincingly demonstrate that embryonic tissues or multicellular aggregates composed of embryonic cells (model tissues) can be characterized in terms of well-defined apparent surface tension that can reproducibly be measured. The biological relevance of these tensions is that they can be used to account for observed morphogenetic tissue configurations as well as quantitatively related to molecular parameters that are difficult to evaluate by other methods. The compression plate tensiometry combined with the solution of the Laplace equation presented here provides a novel, reliable and accurate way to determine interfacial tensions in cases where most classical techniques fail (such as strongly viscous or mutually buoyant liquids) and, to our knowledge, the only method applicable to tissues.

* * *

This work was supported by the National Science Foundation [FIBR-0526854].

REFERENCES

[1] Steinberg M. S., *Science*, **141** (1963) 401.
[2] Steinberg M. and Poole T., *Liquid Behavior of Embryonic Tissues in Cell Behaviour*, edited by Bellairs R., Curtis A. and Dunn G. (Cambridge University Press, Cambridge) 1982, pp. 583–607.
[3] Foty R. A., Pfleger C. M., Forgacs G. and Steinberg M. S., *Development*, **122** (1996) 1611.
[4] Godt D. and Tepass U., *Nature*, **395** (1998) 387.
[5] Gonzalez-Reyes A. and St Johnston D., *Development*, **125** (1998) 3635.
[6] Hayashi T. and Carthew R. W., *Nature*, **431** (2004) 647.

[7] Foty R. A., Forgacs G., Pfleger C. M. and Steinberg M. S., *Phys. Rev. Lett.*, **72** (1994) 2298.
[8] Forgacs G., Foty R. A., Shafrir Y. and Steinberg M. S., *Biophys. J.*, **74** (1998) 2227.
[9] Foty R. A. and Steinberg M. S., *Dev. Biol.*, **278** (2005) 255.
[10] Hegedus B., Marga F., Jakab K., Sharpe-Timms K. L. and Forgacs G., *Biophys. J.*, **91** (2006) 2708.
[11] Phillips H. M., Steinberg M. S. and Lipton B., *Dev. Biol.*, **59** (1977) 124.
[12] du Nouy P. L., *J. Gen. Physiol.*, **7** (1925) 625.